

REVIEW ARTICLE

Open Access

A guide to ^{13}C metabolic flux analysis for the cancer biologist

Maciek R. Antoniewicz¹

Abstract

Cancer metabolism is significantly altered from normal cellular metabolism allowing cancer cells to adapt to changing microenvironments and maintain high rates of proliferation. In the past decade, stable-isotope tracing and network analysis have become powerful tools for uncovering metabolic pathways that are differentially activated in cancer cells. In particular, ^{13}C metabolic flux analysis (^{13}C -MFA) has emerged as the primary technique for quantifying intracellular fluxes in cancer cells. In this review, we provide a practical guide for investigators interested in getting started with ^{13}C -MFA. We describe best practices in ^{13}C -MFA, highlight potential pitfalls and alternative approaches, and conclude with new developments that can further enhance our understanding of cancer metabolism.

Introduction

In the past decade, measuring intracellular metabolism has become an indispensable tool in biomedical research^{1,2}. Cancer metabolism is an especially active area of research^{3–8}. It has long been recognized that cancer cells exhibit rewired metabolism compared to normal cells. A century ago, Warburg⁹ described how cancer cells take up large amounts of glucose and preferentially convert it to lactate, even under aerobic conditions. This so-called Warburg effect, or aerobic glycolysis, is a major hallmark of cancer metabolism^{10–12}. More recently, with the aid of stable-isotope tracers and network analysis, additional metabolic pathways were identified that are activated in cancer cells, including reductive metabolism of glutamine¹³, altered glycolysis¹⁴, serine and glycine metabolism^{15–17}, one-carbon metabolism^{18,19}, transketolase-like 1 (TKTL1) pathway^{20,21}, and acetate metabolism^{22–25}. The activities of these pathways allow cancer cells to extract cellular building blocks and energy from substrates and use them for cell growth. With the rapid progress in cancer research, an increasingly clearer picture is generated how cancer cells rewire their

metabolism, adapt to and manipulate their micro-environment^{26–28}, and maintain a continuous supply of anabolic precursors, reducing equivalents and energy to fuel the reproduction of more cancer cells^{5,29}.

The complexities of mammalian metabolism require a systems-level analysis of the underlying networks and metabolic phenotypes^{30,31}. Currently, ^{13}C metabolic flux analysis (^{13}C -MFA) is the preferred tool for quantitative characterization of metabolic phenotypes in microbial^{32–34} and mammalian cells^{3,4,35–38}. The emergence of ^{13}C -MFA as a primary research tool was made possible in large part due to several major advances in theoretical approaches for conducting ^{13}C -MFA calculations^{39–41}, and more recently, by the availability of dedicated and user-friendly software tools for ^{13}C -MFA such as Metran and INCA^{42,43}. However, ^{13}C -MFA it is still not widely used by cancer biologists, outside of a few expert groups. This may be in part because ^{13}C -MFA is sometimes perceived as unintuitive, obscure, demanding in terms of time and data, and costly in terms of initial capital investment and isotopic tracers. Moreover, few guidelines exist to help researchers get started with ^{13}C -MFA^{44,45}. The main objective of this review is to address these concerns by providing practical guidelines for cancer biologists interested in ^{13}C -MFA. First, we describe the basics of ^{13}C -MFA, discuss key assumptions that are inherent in

Correspondence: Maciek R. Antoniewicz (mranton@udel.edu)

¹Department of Chemical and Biomolecular Engineering, Metabolic Engineering and Systems Biology Laboratory, University of Delaware, Newark, DE 19716, USA

© The Author(s) 2018



Open Access This article is licensed under a Creative Commons Attribution 4.0 International License, which permits use, sharing, adaptation, distribution and reproduction in any medium or format, as long as you give appropriate credit to the original author(s) and the source, provide a link to the Creative Commons license, and indicate if changes were made. The images or other third party material in this article are included in the article's Creative Commons license, unless indicated otherwise in a credit line to the material. If material is not included in the article's Creative Commons license and your intended use is not permitted by statutory regulation or exceeds the permitted use, you will need to obtain permission directly from the copyright holder. To view a copy of this license, visit <http://creativecommons.org/licenses/by/4.0/>.

^{13}C -MFA but may not always be explicitly stated, highlight best practices in ^{13}C -MFA, and identify potential pitfalls as well as alternative approaches. Throughout, we emphasize key aspects that should be considered when planning tracer experiments and performing ^{13}C -MFA calculations to ensure correct interpretation of data and results, and to increase insights obtained from these studies.

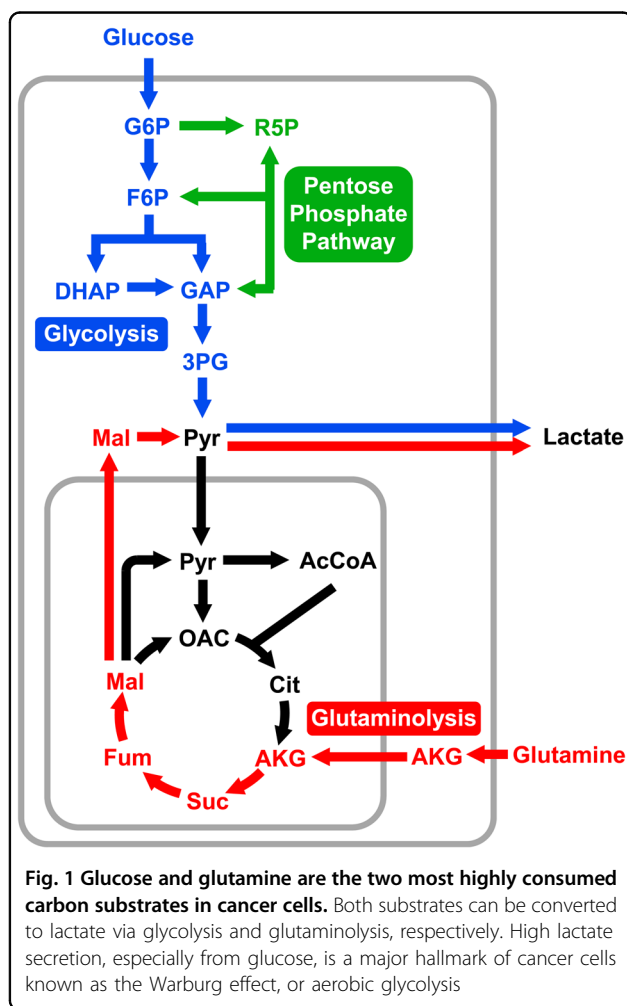
Basics of ^{13}C -MFA

Cellular metabolism serves four important functions in proliferating cancer cells: (1) supply of anabolic building blocks for cell growth; (2) generation of metabolic energy in the form of ATP to drive thermodynamically unfavorable reactions; (3) generation of redox equivalents in the form of NADPH for anabolic processes such as fatty acid biosynthesis and to combat oxidative stress; and (4) maintaining redox homeostasis by oxidizing excess NADH generated in central metabolic pathways.

The first step in obtaining a quantitative picture of cellular metabolism is to measure the growth rate of the cells and quantify nutrient uptake and secretion rates such

as glucose and glutamine uptake and lactate secretion^{46,47} (Fig. 1). These external rates provide important boundary constraints on intracellular pathway activities. However, due to redundancies in mammalian metabolic pathways, external rates alone do not allow detailed conclusions to be drawn about the relative contribution of specific metabolic pathways to overall metabolism^{46,48}. To examine intracellular fluxes in detail, stable isotopes such as ^{13}C are utilized. When a labeled substrate, e.g., [1,2- ^{13}C]glucose, is metabolized by cells, enzymatic reactions rearrange carbon atoms resulting in specific labeling patterns in downstream metabolites that can be measured with analytical techniques such as mass spectrometry (MS), or nuclear magnetic resonance. For a well-selected tracer, different metabolic pathways will produce distinctly different labeling patterns in the measured metabolites from which fluxes can be inferred^{49,50}. However, in most cases, isotopic labeling data cannot be interpreted intuitively due to the highly complex nature of atom rearrangements in metabolic pathways⁵¹; instead, a formal model-based analysis approach is required to extract flux information from the labeling data. In the past 20 years, ^{13}C -MFA has emerged as the primary approach used for converting isotopic labeling data into corresponding metabolic flux maps⁴⁵.

The main objective of ^{13}C -MFA is thus to generate a quantitative map of cellular metabolism by assigning flux values to the reactions in the network model and confidence intervals for each estimated flux (Fig. 2). At a high level, ^{13}C -MFA is formulated as a least-squares parameter estimation problem, where fluxes are unknown model parameters that must be estimated by minimizing the difference between the measured labeling data and labeling patterns simulated by the model, subject to stoichiometric constraints resulting from mass balances for intracellular metabolites and metabolite labeling states, the so-called isotopomers^{40,52}. When ^{13}C -MFA first emerged in 1990s⁵³, the main challenge was to develop efficient algorithms for solving large sets of isotopomer mass balances⁵⁴. Eventually, the computational problems in ^{13}C -MFA were resolved with the development of the elementary metabolite unit (EMU) framework that allows efficient simulation of isotopic labeling in any arbitrary biochemical network model³⁹. The EMU framework was subsequently incorporated into user-friendly software tools for ^{13}C -MFA, such as Metran and INCA^{42,43}, that are freely available to the scientific community. These powerful tools have opened up ^{13}C -MFA to a much wider scientific audience, including cancer biologists, that may not have extensive background in mathematics and statistics, which was required before these software packages became available. In the next sections, we describe in detail the three inputs that are required for performing ^{13}C -MFA calculations: (i)



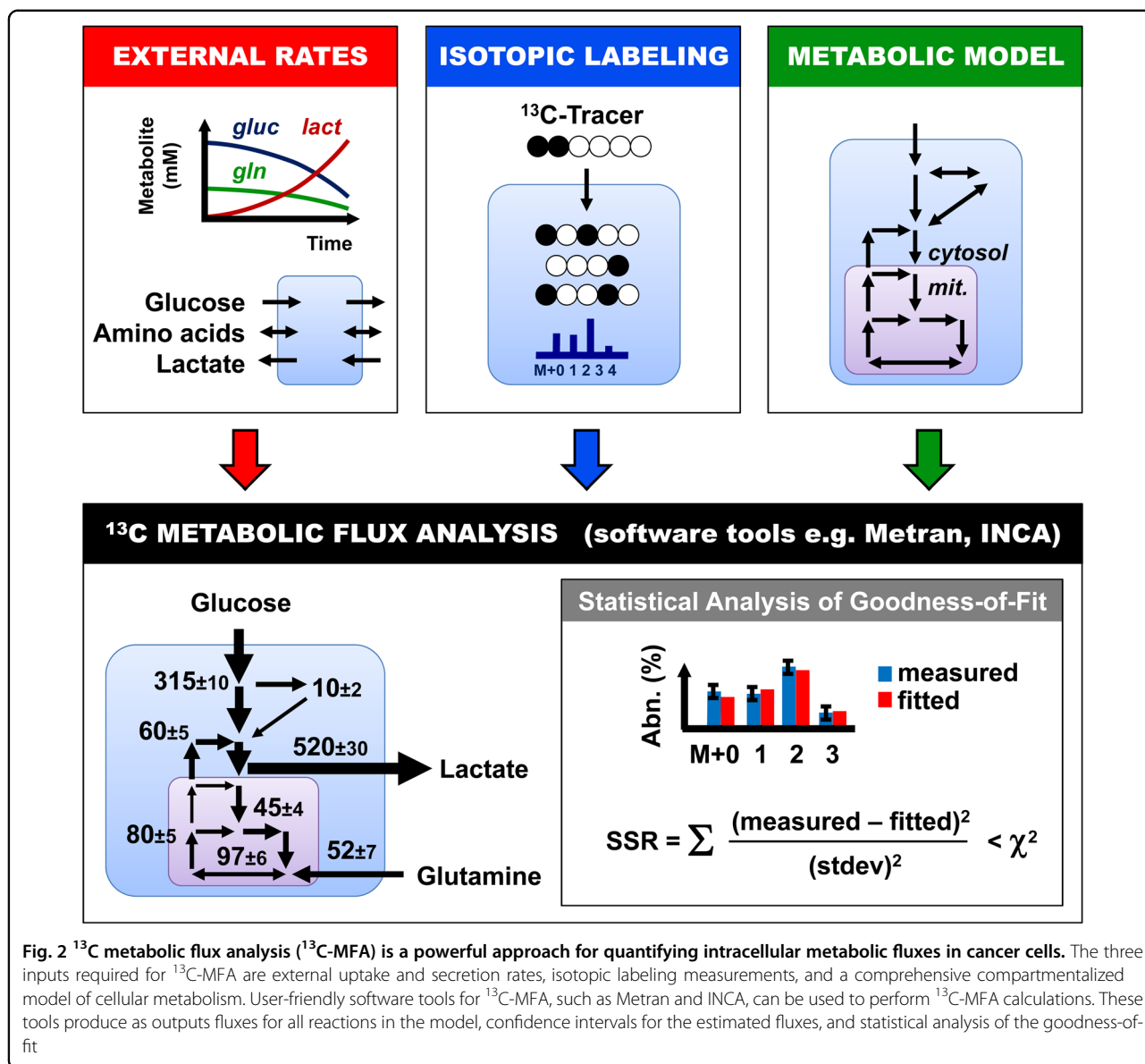


Fig. 2 ¹³C metabolic flux analysis (¹³C-MFA) is a powerful approach for quantifying intracellular metabolic fluxes in cancer cells. The three inputs required for ¹³C-MFA are external uptake and secretion rates, isotopic labeling measurements, and a comprehensive compartmentalized model of cellular metabolism. User-friendly software tools for ¹³C-MFA, such as Metran and INCA, can be used to perform ¹³C-MFA calculations. These tools produce as outputs fluxes for all reactions in the model, confidence intervals for the estimated fluxes, and statistical analysis of the goodness-of-fit

external rates; (ii) isotopic labeling; and (iii) metabolic model (Fig. 2).

Determination of external rates

To quantify intracellular metabolic fluxes, first, the cross talk between the cells and their environment must be quantified. Collectively referred to as external rates, this includes measuring influxes of nutrients such as glucose and glutamine, and secretion of metabolic by-products such as lactate and glutamate. In addition, the rate of cell growth must be determined. Assuming cells are continuously dividing, the cell number will increase exponentially according to:

$$N_x = N_{x,0} \cdot \exp(\mu \cdot t) \tag{1}$$

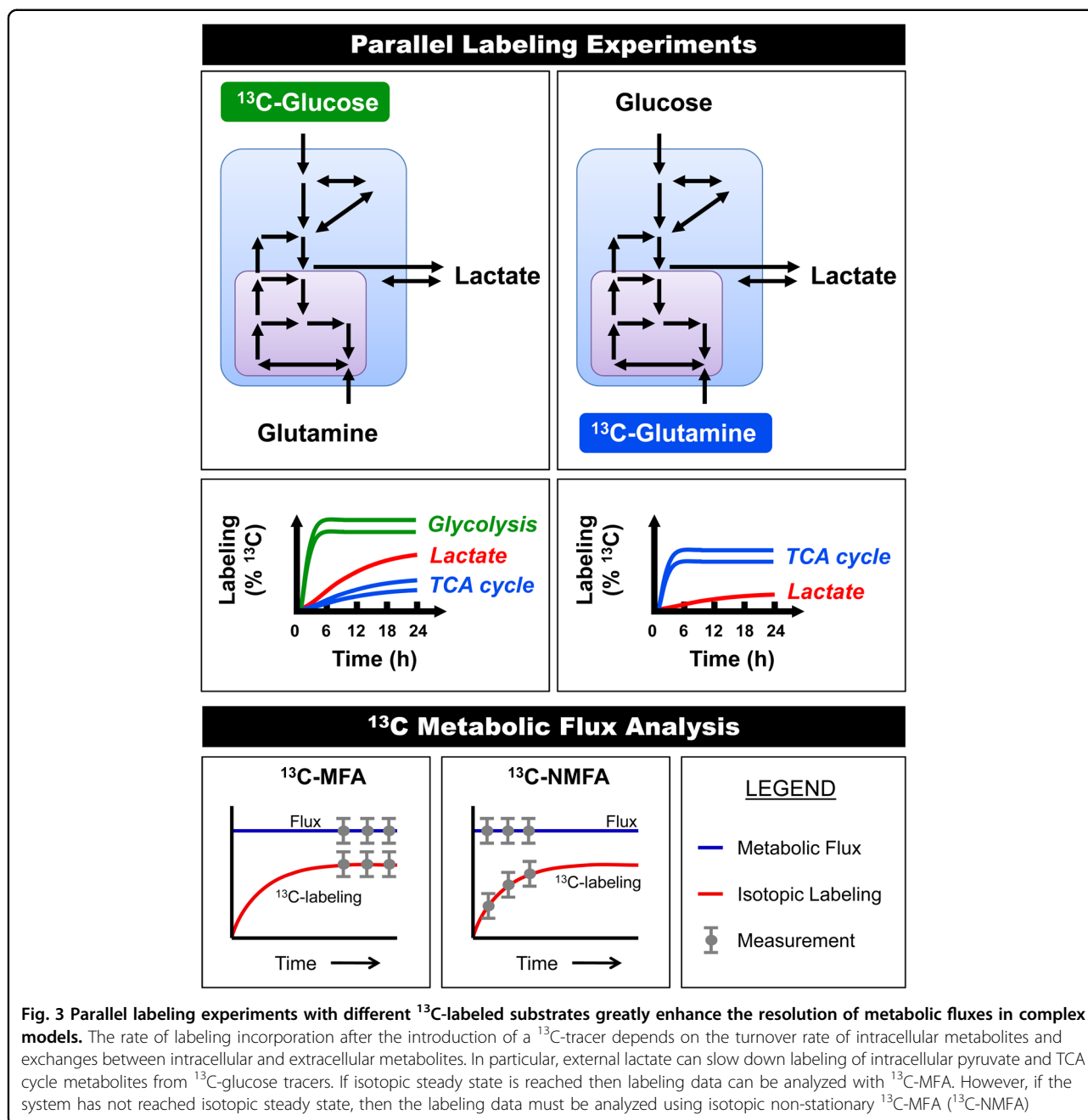
Here N_x is the number of cells (typically expressed in millions of cells), and μ (1/h) is the growth rate. The growth rate is easily determined by plotting the natural logarithm of N_x vs time and determining the slope of the curve. If cells are counted only at two time points, then the growth rate is determined as follows:

$$\mu = \frac{\ln(N_{x,t2}) - \ln(N_{x,t1})}{\Delta t} \tag{2}$$

The doubling time (t_d) is inversely related to the growth rate, according to:

$$t_d = \ln(2)/\mu \tag{3}$$

External rates, i.e., nutrient uptake rates and waste product secretion rates, can be determined in a



straightforward way by measuring changes in metabolite concentrations during the labeling experiment. For exponentially growing cells, external rates (r_b in units $\text{nmol}/10^6 \text{ cells}/\text{h}$) can be calculated as follows:

$$r_i = 1000 \cdot \frac{\mu \cdot V \cdot \Delta C_i}{\Delta N_x} \quad (4)$$

Here ΔC_i (mmol/L) is the change in concentration of a particular metabolite i between two sampling time points, ΔN_x is the change in cell number (expressed in millions of cells) during the same time period, V (mL) is the culture

volume, and μ (1/h) is the growth rate. Based on this expression, external rates have negative values for uptake rates and positive values for secretion rates. For non-proliferating cells, external rates are determined by a slightly different expression:

$$r_i = 1000 \cdot \frac{V \cdot \Delta C_i}{\Delta t \cdot N_x} \quad (5)$$

Because glutamine is an unstable molecule, i.e., it spontaneously degrades to pyroglutamate and ammonium under normal culture conditions, the calculated

glutamine uptake rate must be corrected for glutamine degradation, i.e., the measured rate reflects both net uptake of glutamine by the cells and glutamine degradation. Glutamine degradation can be expressed as a first-order degradation process with a degradation constant of around 0.003/h⁵⁵. After correcting for glutamine degradation⁵⁵, the true net glutamine uptake rate is obtained. For long tracer experiments (e.g., >24 h), it may also be necessary to correct for evaporation effects. For this purpose, control experiments without cells are performed. By measuring the apparent increases in metabolite concentrations over time, the rate of evaporation can be estimated. The dynamics of glutamine degradation are also easily determined from these control experiments.

For ¹³C-MFA studies, external rates are often determined for glucose uptake, lactate secretion, and amino acid uptake and secretion. For proliferating cancer cells, typical values are as follows: 100–400 nmol/10⁶ cells/h for glucose uptake; 200–700 nmol/10⁶ cells/h for lactate secretion; 30–100 nmol/10⁶ cells/h for glutamine uptake; and 2–10 nmol/10⁶ cells/h for uptake or secretion of other amino acids. Depending on the scope of the study, it may also be important to measure the rates of other metabolites such as ammonium, pyruvate, acetate, citrate, and any other significant nutrients or by-products that cancer cells exchange with their environment.

Measurement of isotopic labeling

When conducting ¹³C-tracer experiments, a labeled substrate is introduced to the culture medium that is then taken up by the cells and metabolized through various metabolic pathways. It takes a certain amount of time before intracellular metabolites reach a constant labeling state, which is referred to as isotopic steady state⁴⁶ (Fig. 3). The time required to reach isotopic steady state depends on the turnover rate of metabolites in a pathway and the labeling dynamics of upstream metabolites that feed into the pathway. The turnover rate of a metabolite pool is roughly equivalent to the ratio of the metabolite pool size and the flux through that metabolite pool. For proliferating cells, isotopic steady state can be reached relatively quickly, i.e., within a few hours after the introduction of the isotopic tracer⁵⁶. However, in some cases, due to exchange of intracellular and external metabolites, significantly slower labeling incorporation rates can be observed. In particular, external lactate often acts as a large buffer that slows down labeling of intracellular pyruvate and downstream metabolic pathways, e.g., tricarboxylic acid (TCA) cycle, when ¹³C-glucose tracers are used⁵⁵. Slow labeling may be observed even if there is large net secretion of lactate, since external lactate readily exchanges with intracellular lactate, which in turn rapidly equilibrates with cytosolic pyruvate. The effective pool size of intracellular pyruvate thus becomes the

combined pool of intracellular pyruvate, intracellular lactate, and external lactate. This buffering effect can be so extreme that certain metabolites may never reach isotopic steady state⁵⁵. One strategy to reduce the buffering effect of lactate is to ensure that little or no lactate is present in the medium at the beginning of ¹³C-glucose tracer experiments.

An important inherent assumption of ¹³C-MFA calculations is that all metabolites are at isotopic steady state. It is thus critical to validate this assumption for all tracer experiments performed. To validate this, isotopic labeling is measured for at least two time points, e.g., 18 and 24 h, after the introduction of tracer. If isotopic labeling is identical for the two time points, then isotopic steady state is confirmed and the labeling data can be analyzed using classical ¹³C-MFA. However, if isotopic labeling is changing with time, then the data must be analyzed using a more advanced ¹³C-MFA approach called isotopic-non-stationary ¹³C-MFA, or ¹³C-NMFA⁴¹. Most software packages for ¹³C-MFA can only perform classical ¹³C-MFA calculations, i.e., assuming isotopic steady state, although a few software packages such as INCA can perform both ¹³C-MFA and ¹³C-NMFA calculations⁴³.

MS is currently the preferred analytical technique used for measuring isotopic labeling of intracellular metabolites. With the technological advances in gas chromatography/MS (GC/MS) and liquid chromatography/MS (LC/MS) in the past two decades, it is now possible to measure mass isotopomer distributions for a large number of intracellular metabolites from as few as one million cells, including for intermediates of glycolysis pathway: fructose 6-phosphate (F6P), dihydroxyacetone phosphate, glycerol 3-phosphate, 3-phosphoglycerate (3PG), phosphoenolpyruvate, pyruvate, and lactate; intermediates of the pentose phosphate pathway (PPP; LC/MS mainly): xylulose 5-phosphate (X5P), ribose 5-phosphate (R5P), and sedoheptulose 7-phosphate; intermediates of the TCA cycle: citrate, α -ketoglutarate (AKG), succinate, fumarate, and malate; and most amino acids, including alanine, aspartate, glutamate, glutamine, proline, serine, and glycine.

Parallel labeling experiments

The selection of an isotopic tracer (or multiple tracers) is one of the most important considerations when designing ¹³C-MFA studies, since this ultimately determines the quality (i.e., precision and accuracy) of flux results that can be obtained⁵⁰. It is now well-known that there is no single best tracer for ¹³C-MFA studies. Generally, ¹³C-glucose tracers are best for determining fluxes in upper metabolism (e.g., glycolysis and PPP), while ¹³C-glutamine tracers typically produce better resolution of fluxes in lower parts of metabolism (e.g., TCA cycle and reductive carboxylation)^{57,58} (Fig. 3). A powerful approach

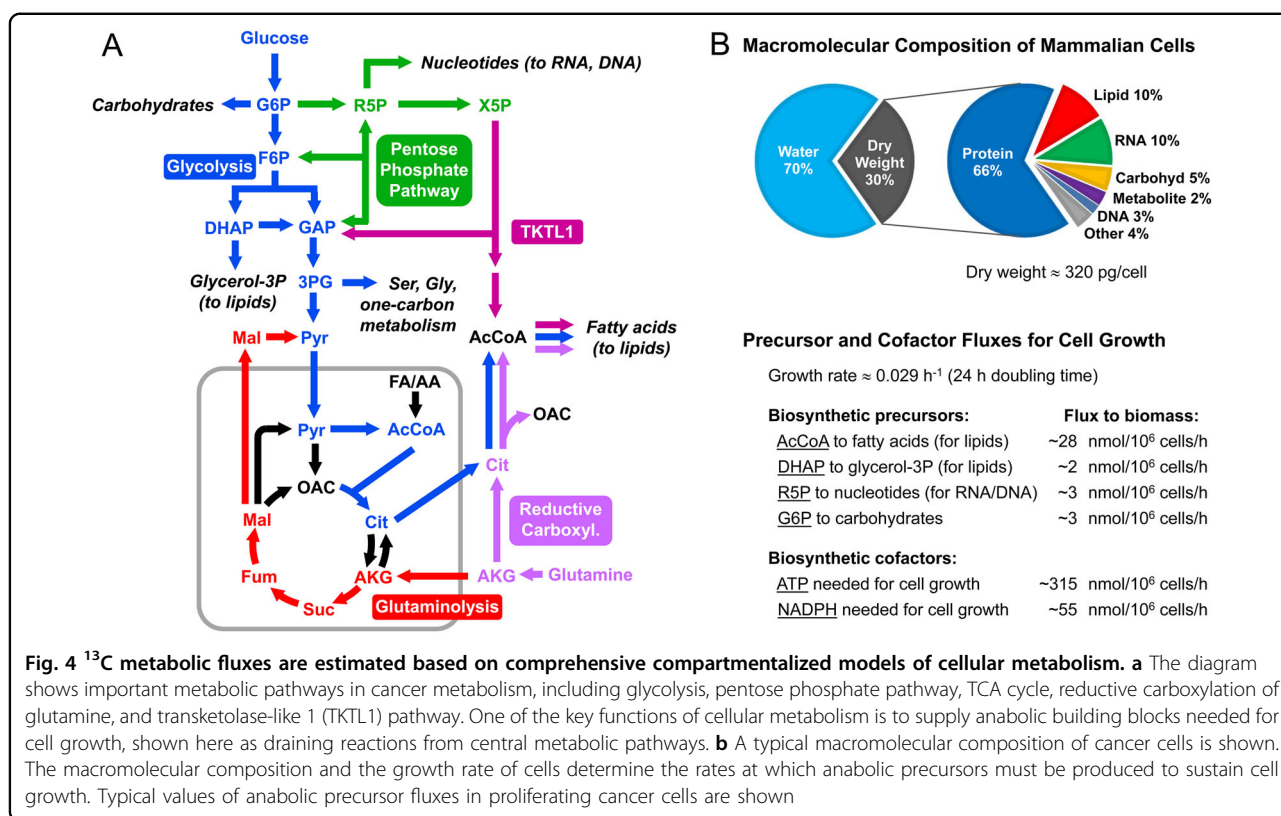


Fig. 4 ¹³C metabolic fluxes are estimated based on comprehensive compartmentalized models of cellular metabolism. **a** The diagram shows important metabolic pathways in cancer metabolism, including glycolysis, pentose phosphate pathway, TCA cycle, reductive carboxylation of glutamine, and transketolase-like 1 (TKTL1) pathway. One of the key functions of cellular metabolism is to supply anabolic building blocks needed for cell growth, shown here as draining reactions from central metabolic pathways. **b** A typical macromolecular composition of cancer cells is shown. The macromolecular composition and the growth rate of cells determine the rates at which anabolic precursors must be produced to sustain cell growth. Typical values of anabolic precursor fluxes in proliferating cancer cells are shown

to achieve high resolution of multiple metabolic pathways is to perform parallel labeling experiments with different tracers and then integrate all data into a single comprehensive flux model^{59,60}. For example, parallel labeling experiments with [1,2-¹³C]glucose and [U-¹³C]glutamine have been demonstrated to be particularly informative and complementary^{56,58,61}. When conducting parallel labeling experiments, it is important that the only difference between the experiments is which metabolite is labeled, i.e., concentrations of all nutrients in the media must be the same for parallel labeling experiments⁶². With recent advances in ¹³C-MFA methodology it is now fairly straightforward to analyze isotopic labeling data from parallel labeling experiments⁴⁵. The Metran software was the first tool that allowed comprehensive analysis of parallel labeling experiments for high-resolution ¹³C-MFA. Recently, other ¹³C-MFA software packages have also included this feature.

Metabolic model for ¹³C-MFA

All ¹³C-MFA calculations are based on a model of biochemical reactions within a specified metabolic network. Determining the scope of the model is an important decision in ¹³C-MFA studies. Unfortunately, there is only limited consensus in the literature on the optimal scope of metabolic models for flux analysis in cancer cells. This is in part due to the fact that the appropriate model

complexity will depend to some degree on the specific choice of isotopic tracer (or tracers), how many parallel labeling experiments are performed, and how many and which labeling measurements are collected. In general, more comprehensive data sets, i.e., based on multiple parallel labeling experiments with different labeled substrates^{36,56,60,63}, will permit the use of more complex models for ¹³C-MFA than smaller data sets obtained using a single tracer experiment.

Typically, ¹³C-MFA models will include all major metabolic pathways of central carbon metabolism such as glycolysis, PPP, TCA cycle, as well as any relevant reactions that connect these pathways (Fig. 4a). Compartmentalization of metabolites and metabolic reactions is an important feature of mammalian cells that must be captured in the model. Metabolites and reactions are therefore assigned to specific metabolic compartments such as cytosol or mitochondrion. Certain metabolites will be present in multiple compartments, for example, pyruvate, acetyl coenzyme A, citrate, malate, fumarate, oxaloacetate, and AKG. These metabolites are treated as separate entities in the model that can have different labeling states in different compartments. Transport reactions in the model allow specific metabolites to be transferred between cellular compartments. Compartment-specific isozymes, which can operate independently, must be included as separate reactions in the model (e.g., cytosolic

and mitochondrial isocitrate dehydrogenases; and cytosolic and mitochondrial malic enzymes). Finally, ^{13}C -MFA models will include a lumped biomass formation reaction that drains anabolic precursors from central metabolism (and extracellular medium, e.g., essential amino acids) for the biosynthesis cellular macromolecules⁵⁵. The stoichiometric coefficients for this lumped biomass reaction are easily determined based on the macromolecular composition of cells (Fig. 4b). Recently, a number of GC/MS-based protocols have been developed that allow biomass compositions of cells to be determined easily and accurately^{64–66}. Typical values for anabolic precursor effluxes for proliferating cancer cells are shown in Fig. 4b.

^{13}C -MFA and statistical analysis

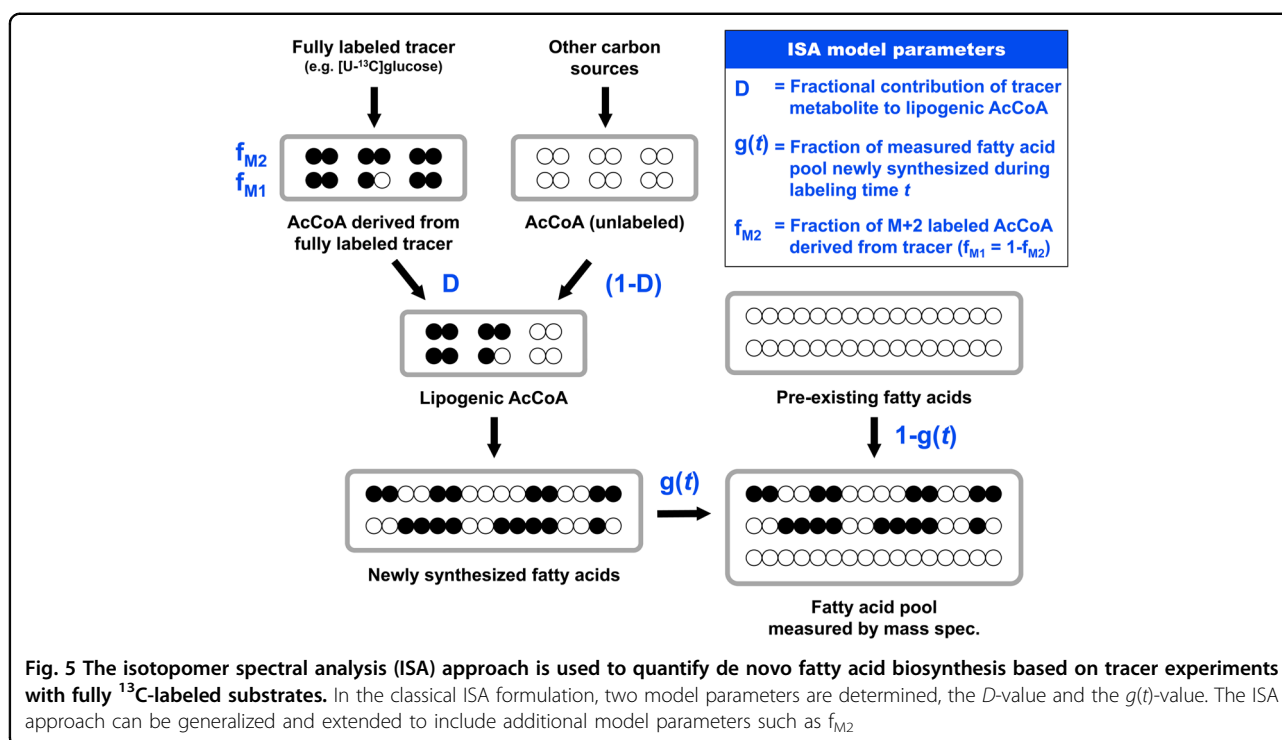
Current software tools for ^{13}C -MFA such as Metran and INCA are designed so that users are not required to have any extensive background in mathematics, statistics, or writing computer code. All of the complex math associated with performing ^{13}C -MFA computations is hidden from the user. These software tools accept as inputs: (1) a user-defined metabolic network model consisting of biochemical reactions and corresponding atom transitions; and (2) a set of measurements consisting of isotopic labeling data and external rates. As outputs, the software returns the following: (1) metabolic fluxes for the entire network; (2) confidence intervals for all estimated fluxes; and (3) statistical analysis of the goodness-of-fit (Fig. 2).

^{13}C -MFA should be viewed as an iterative process that requires careful scrutiny of the analysis results. After the software returns a result, it is up to the user to determine how acceptable the result is, and this requires some level of experience. Generally, it is rare that the first result returned by the software will be the optimal solution. There are several important reasons for this. First, as mentioned in the introduction, in ^{13}C -MFA a highly nonlinear multi-dimensional parameter estimation problem is solved⁴⁰. Problems of this kind have many sub-optimal local solutions, and there is no guarantee that the first solution returned by the software will be the global optimal solution. To address this concern, ^{13}C -MFA is typically restarted many times with random initial values for all fluxes and the goodness-of-fit of these iterations is compared. The goodness-of-fit is expressed by the sum of squared weighted residuals, or the SSR value⁴⁰ (Fig. 2). The lower the SSR value, the better the agreement between the measured data and the model fit. Assuming that the metabolic model is correct and data are without gross measurement errors, the minimized SSR is a stochastic variable with a χ^2 -distribution. Based on this property, it is possible to calculate a maximum statistically acceptable value for SSR, which is roughly equal to the number of fitted measurements (n) minus the number of estimated independent parameters (p). More technically,

the acceptable range of SSR values is between $\chi^2_{\alpha/2}(n-p)$ and $\chi^2_{1-\alpha/2}(n-p)$, where α is a certain chosen threshold value, for example, 0.05 for the 95% confidence interval.

The strategy for performing ^{13}C -MFA is thus to restart flux estimation many times (typically at least 10 times, but more is preferred) and compare the SSR values. The solution with the lowest SSR value is then selected as the optimal solution. Often, multiple iterations will produce the same low SSR value, which increases the likelihood that the solution is indeed the global optimal solution. In practice, however, it is not uncommon that the lowest SSR value obtained in this way is still greater than the maximum statistically allowed SSR. Some common reasons for this are as follows:

1. Errors in the metabolic model. Mistakes in the user-specified metabolic model such as incorrect reaction stoichiometries or errors in atom transitions are generally easy to identify and correct.
2. Incomplete metabolic model. Omitting important reactions or pathways from the model will result in poor fits. Thus, depending on the quality of fit, the scope of the model may need to be adjusted. In some cases, it may be necessary to include hypothetical reactions in the model in order to achieve an acceptable fit. In this way, ^{13}C -MFA can be used as a hypothesis generating tool that can eventually lead to the discovery of novel metabolic pathways or reactions^{67–72}. As an example, the TKTL1 pathway was recently discovered in Chinese hamster ovary cells by this approach⁷³.
3. Gross measurement errors. It is not uncommon that certain labeling data will contain gross measurement errors, for example, due to co-elution of metabolites in GC/MS and LC/MS analyses. Careful inspection of ion chromatograms can in most cases help to identify co-elution problems. In such cases, labeling data for the contaminated metabolite fragments should be excluded from flux analysis.
4. Incorrect assumptions about measurement errors. The SSR value is calculated by summing up the weighted squared differences between the measured and simulated values. The weighting factors are inverses of measurement standard deviations squared. The assumed measurement errors thus greatly influence the calculated SSR value. Typical measurement errors used in ^{13}C -MFA studies are as follows: 0.004 (or 0.4 mol%) for GC/MS data; 0.01 (or 1 mol%) for LC/MS data; and 5–10% relative error for external rates. In cases when very high or very low SSR values are obtained, it may be necessary to reevaluate the assumptions regarding measurement errors. Moreover, inspection of weighted residuals can inform if correct measurement errors have been assigned. Assuming



measurement errors are random, the weighted residuals should follow a normal distribution $N(\mu = 0, \sigma^2 = 1)$, which can be easily tested⁴⁰.

Isotopomer spectral analysis

Isotopomer spectral analysis (ISA) is a related and widely used analysis approach for analyzing de novo fatty acid biosynthesis⁷⁴ (Fig. 5). ISA calculations can be performed with most current software tools for ^{13}C -MFA. Initially developed in early 1990s (before the ^{13}C -MFA approach was fully formalized), the ISA approach is based on a relatively simple two-parameter model for analyzing mass isotopomer distributions of fatty acids from tracer experiments with fully ^{13}C -labeled substrates, e.g., $[\text{U}-^{13}\text{C}]$ glucose. In the classical ISA formulation, two model parameters are determined: the D -value and the $g(t)$ -value⁷⁴. The D -value quantifies the fractional contribution of the fully ^{13}C -labeled metabolite to lipogenic AcCoA, and the $g(t)$ -value quantifies the fraction of fatty acids that were newly synthesized during the labeling time t .

Typically, several parallel labeling experiments are performed with different fully ^{13}C -labeled substrates, e.g., $[\text{U}-^{13}\text{C}]$ glucose and $[\text{U}-^{13}\text{C}]$ glutamine, and isotopic labeling is measured for multiple fatty acids in each experiment, e.g., C16:0, C16:1, C18:0, and C18:1, using GC/MS. In theory, for a given tracer the D -values should be identical for all fatty acids, since all fatty acids are derived from the same cytosolic AcCoA pool. In contrast, the $g(t)$ -values may be different for each fatty acid since

different fatty acids may be synthesized at different rates. However, $g(t)$ -values for a particular fatty acid determined with different tracers, e.g., with $[\text{U}-^{13}\text{C}]$ glucose and $[\text{U}-^{13}\text{C}]$ glutamine, should be the same since the synthesis rate of a particular fatty acid should not depend on which substrate is labeled. The ISA approach can be generalized for analysis of odd-chain fatty acids, e.g., C15:0 and C17:0, as was recently demonstrated⁶². Moreover, ISA can be extended to include additional model parameters⁶² (Fig. 5). In the classical ISA model, it is assumed that fully labeled substrates, e.g., $[\text{U}-^{13}\text{C}]$ glutamine, will produce only fully labeled AcCoA (i.e., M + 2-labeled). However, this assumption may not always be valid. For example, metabolism of $[\text{U}-^{13}\text{C}]$ glutamine in the TCA cycle can result in some loss of ^{13}C , which will produce a mixture of M + 1- and M + 2-labeled AcCoA. Moreover, catabolism of certain substrates such as $[\text{U}-^{13}\text{C}]$ leucine will always produce a mixture of M + 1- and M + 2-labeled AcCoA due to carbon exchange with unlabeled CO_2 ⁷⁵. For example, for the case of $[\text{U}-^{13}\text{C}]$ leucine, 33% of AcCoA will be M + 1-labeled and 67% of AcCoA will be M + 2-labeled⁶². By including an additional f_{M2} parameter in the ISA model, losses of ^{13}C atoms can be captured, which produces more accurate estimates of D - and $g(t)$ -values.

As indicated above, ISA analysis is typically performed with different fully ^{13}C -labeled substrates in parallel experiments. These studies provide important insights into the relative contributions of different nutrients for de novo lipogenesis^{13,76}. The estimated $g(t)$ -values are also

informative, since they can be used to calculate absolute de novo biosynthesis rates of fatty acids (nmol/10⁶ cells/h):

$$\text{Fatty acid biosynthesis rate} = \frac{\text{FA}}{t} \cdot \frac{g(t)}{1 - g(t)} \quad (6)$$

Here FA is the macromolecular content of a particular fatty acid in cancer cells (in units nmol/10⁶ cells; a typical value for palmitate is 40 nmol/10⁶ cells), and Δt (h) is the length of the tracer experiment. The fatty acid content of cancer cells is easily determined with GC-flame ionization detector, or using the protocols described by Long and Antoniewicz⁶⁵.

Quantifying fluxes in upper metabolism

In the next two sections, we describe briefly common stable-isotope tracing strategies for determining fluxes in upper and lower parts of central carbon metabolism, respectively. When performing flux analysis in upper metabolism, the drain of metabolic precursors toward biomass synthesis such as glucose 6-phosphate (G6P) for carbohydrates, R5P for nucleotides, and glycerol 3-phosphate for lipids can be generally ignored, since the glucose uptake rate (~100–400 nmol/10⁶ cells/h) is typically two orders of magnitude greater than the drain of anabolic precursors for cell growth (~2–3 nmol/10⁶ cells/h; Fig. 4). However, when performing flux analysis in lower metabolism, the drain of AcCoA for lipogenesis (~28 nmol/10⁶ cells/h) cannot be ignored since this flux is comparable in magnitude to other fluxes in lower metabolism.

At present, [1,2-¹³C]glucose is one of the most widely used tracers to quantify fluxes of glycolysis and PPP (Fig. 6a). With this tracer the two pathways produce distinctly different labeling patterns in downstream metabolites such as 3PG, which can be easily measured with GC/MS and LC/MS. Metabolism of glucose via glycolysis produces 3PG that is 50% M + 2-labeled and 50% unlabeled (i.e., M + 0), while metabolism of glucose via oxidative PPP (oxPPP) produces a mixture of M + 0-, M + 1-, and M + 2-labeled 3PG. For a single pass through oxPPP, the labeling of 3PG is 60% M + 0, 20% M + 1, and 20% M + 2. The ratio of M + 1/M + 2 mass isotopomers of 3PG thus roughly approximates the relative contribution of oxPPP to glucose metabolism. However, this approximation should be used with caution. Specifically, the reversible G6P isomerase reaction, which interconverts G6P and F6P, can reroute a significant fraction of F6P that is produced via PPP back to G6P to be metabolized via oxPPP a second time (and possibly a third time), which results in additional losses of ¹³C (Fig. 6a). Thus, depending on the equilibration of F6P and G6P, the M + 1 and M + 2 mass isotopomers of 3PG can be significantly <20% and the ratio M + 1/M + 2 may be

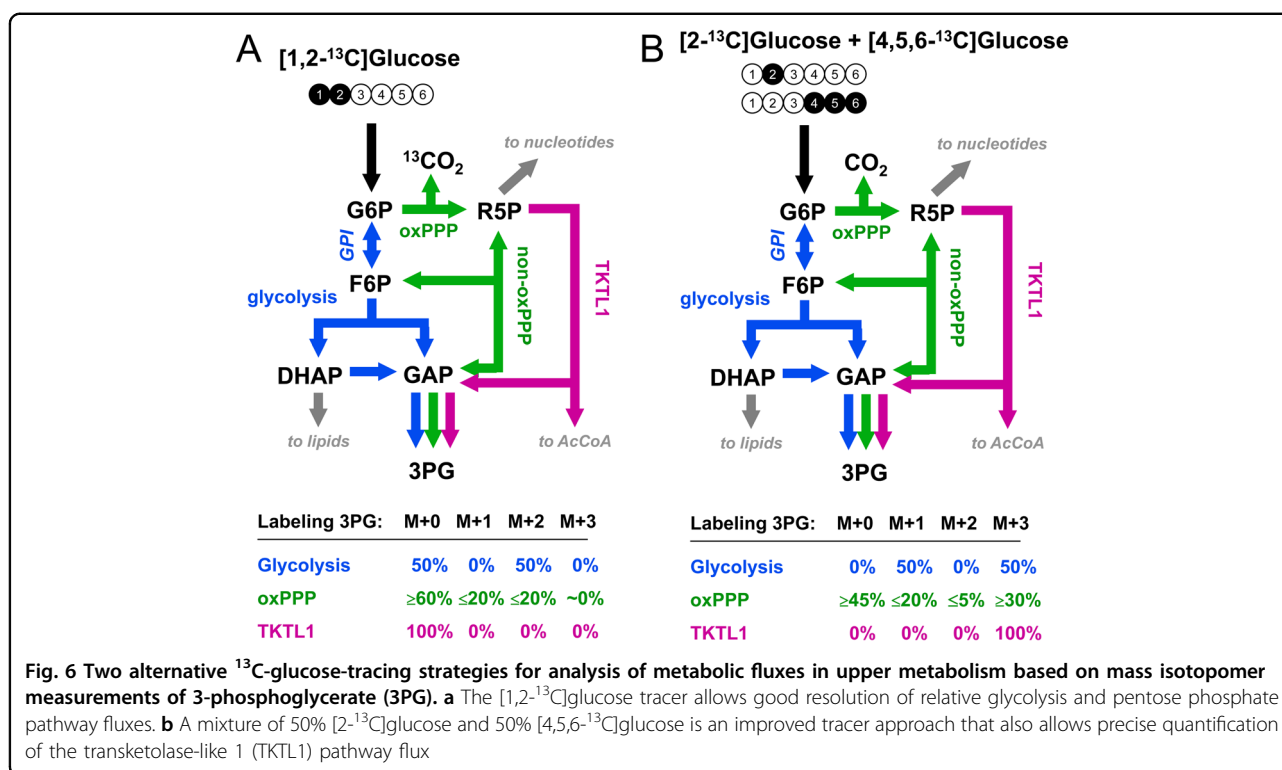
different from unity. Thus, to obtain a reliable estimate of oxPPP flux, the 3PG labeling data should be analyzed formally with ¹³C-MFA.

Recently, a third metabolic pathway was discovered in cancer cells by which glucose can be metabolized, the TKTL1 pathway, which converts X5P (an intermediate of PPP) to glyceraldehyde 3-phosphate and a two-carbon metabolite, likely acetate, which can be further metabolized to cytosolic AcCoA^{20,21} (Fig. 6). Unfortunately, [1,2-¹³C]glucose and several other commonly used glucose tracers cannot provide a reliable estimate of the TKTL1 flux. To address this limitation, alternative glucose-tracing strategies have been developed to better resolve the three glucose metabolism pathways, glycolysis, PPP, and TKTL1⁷³. One of the best tracer strategies was based on mixtures of 50% [4,5,6-¹³C]glucose and 50% of either [1-¹³C]glucose, [2-¹³C]glucose, or [3-¹³C]glucose (Fig. 6b). With these tracers, it is possible to determine precise fluxes of all three metabolic pathways, as recently demonstrated in Chinese hamster ovary cells⁷³. Other optimal glucose tracers have also been proposed for analysis of specific metabolic pathways; for example, [3,4-¹³C]glucose was determined to be a particularly good tracer for quantifying the anaplerotic flux of glucose into the TCA cycle^{57,77,78}.

Quantifying fluxes in lower metabolism

For analysis of fluxes in lower part of central carbon metabolism, i.e., downstream of pyruvate, fully labeled [U-¹³C]glutamine is often used. Glutamine is the second most highly consumed carbon substrate by many cancer cells (after glucose)⁷⁹; as a result, [U-¹³C]glutamine produces high labeling in metabolites, especially in TCA cycle intermediates, and rich labeling patterns for flux estimation using ¹³C-MFA (Fig. 7). Another advantage of using ¹³C-glutamine as a tracer is that labeling dynamics of ¹³C-glutamine are not affected by the buffering effect of extracellular lactate. Since ¹³C-glutamine labels mainly metabolites downstream of pyruvate, isotopic steady state is reached for the labeled TCA cycle metabolites within a few hours after [U-¹³C]glutamine addition, even when external lactate concentration is high⁵⁶.

In the past decade, [U-¹³C]glutamine tracing has played an important role in elucidating the contribution of glutamine to lipogenesis via reductive carboxylation pathway^{13,42}, i.e., via the conversion of glutamine to AKG, then to citrate (i.e., in the reverse direction of TCA cycle, catalyzed by isocitrate dehydrogenases), and finally to AcCoA after cleavage by ATP citrate lyase. To highlight additional flux information that can be obtained from [U-¹³C]glutamine tracer experiments, Fig. 7 shows schematically the flow isotopic labeling from [U-¹³C]glutamine into relevant metabolic pathways. The insert in Fig. 7 shows an example of labeling data set obtained from

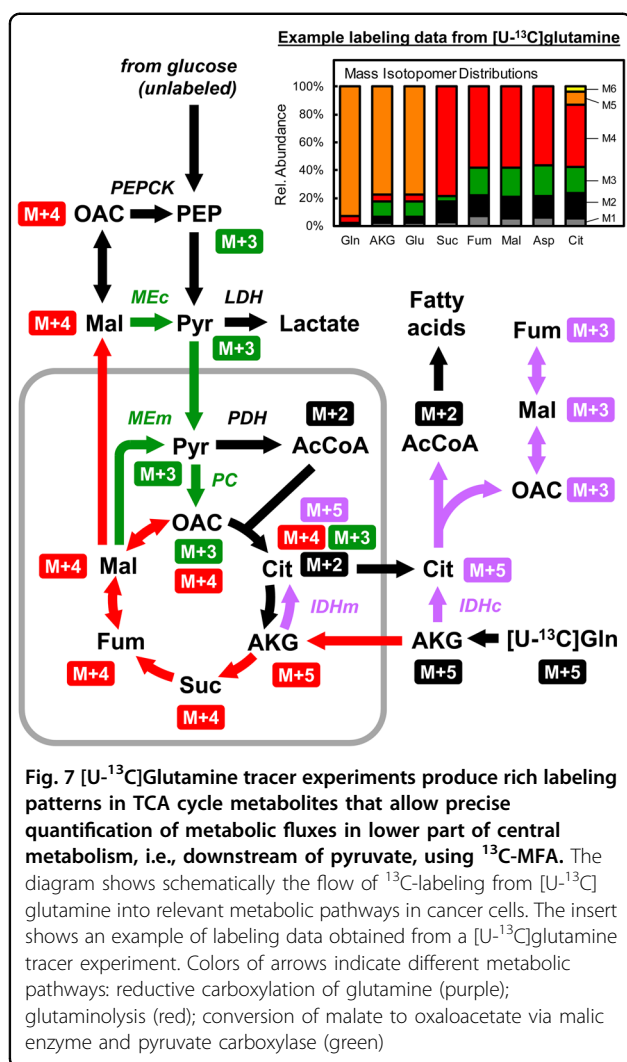


a [U-¹³C]glutamine tracer experiment. Metabolism of [U-¹³C]glutamine via reductive carboxylation (purple arrows in Fig. 6) results in the production of M + 5-labeled citrate⁴²; after cleavage of citrate by ATP citrate lyase, M + 2-labeled AcCoA and M + 3-labeled oxaloacetate are produced (while labeling of oxaloacetate cannot be measured directly, it can be inferred from the labeling of aspartate). In contrast, metabolism of [U-¹³C]glutamine via the glutaminolysis pathway along the normal oxidative direction of the TCA cycle (red arrows in Fig. 6) results in the production of M + 4-labeled succinate, fumarate, malate, and oxaloacetate. M + 4 malate can also produce M + 3-labeled oxaloacetate, after conversion to pyruvate via malic enzyme, followed by carboxylation of pyruvate to oxaloacetate by pyruvate carboxylase (green arrows in Fig. 6). Taken together, [U-¹³C]glutamine tracer experiments produce rich labeling patterns in TCA cycle metabolites that permit precise quantification of metabolic fluxes in these pathways using ¹³C-MFA. In addition to [U-¹³C]glutamine, [5-¹³C]glutamine and [1-¹³C]glutamine have also been used for ¹³C-MFA^{13,36,77}. However, in general, these singly labeled glutamine tracers are not as informative as [U-¹³C]glutamine for comprehensive analysis of cellular metabolism.

Concluding remarks

The isotopic tracing strategies and ¹³C-MFA methods reviewed here present powerful tools for elucidating

metabolic flux rewiring in cancer cells. Technically, other stable isotopes such as ²H, ¹⁸O, and ¹⁵N can also be used to study metabolic phenotypes, and for certain applications these alternative isotope tracers may be preferred^{80,81}. From a modeling perspective, the application of multiple isotopes will not cause any problems for MFA. In fact, one of the motivations for developing the EMU framework was to permit and encourage the application of multiple isotopes for flux analysis³⁹. Several pioneering studies have already made use of this^{45,82}. However, there are several drawbacks and limitations that should be considered when contemplating the use of alternative stable isotopes. For example, ¹⁸O tracers are generally much more expensive than ¹³C tracers and at present the number commercially available ¹⁸O tracers is limited. While ¹⁵N can be used to investigate metabolic pathways where the metabolic intermediates contain N atoms, such as amino-acid pathways, they cannot be used to study central carbon metabolism. Finally, interpretation of ²H labeling data is complicated by the presence of significant deuterium kinetic isotope effects. In contrast to ¹³C tracers, where it has been demonstrated that the kinetic isotope effects are negligible⁸³, the kinetic isotope effects for ²H are substantial⁸⁴. Thus, determining fluxes from ²H labeling data is strongly influenced by specific assumptions made regarding the magnitude of kinetic isotope effects for various enzymatic reactions. Still, ²H tracers can be valuable in resolving specific aspects of



metabolism such as NADPH metabolism in different cellular compartments, which cannot be elucidated with ¹³C tracers^{85,86}.

Currently, one of the biggest challenges for ¹³C-MFA in mammalian cells is to resolve compartment-specific fluxes⁸⁷. While certain compartment-specific metabolic fluxes can be determined precisely with ¹³C-MFA, e.g., mitochondrial vs cytosolic malic enzyme fluxes, other fluxes are much more difficult to resolve, e.g., mitochondrial vs cytosolic isocitrate dehydrogenase fluxes. In theory, resolving compartment-specific fluxes would be easier if compartment-specific labeling data could be collected⁸⁸. However, with current protocols for quenching metabolism and extracting intracellular labeling, all intracellular metabolite pools are sampled. As a result, the measured labeling data must be modeled as mixtures from multiple cellular pools^{36,61,89}. To resolve compartmentalized metabolism, alternative approaches

such as organelle isolation may be valuable in the future^{90–92}.

When interpreting ¹³C-MFA results, it is also important to keep in mind that the accuracy of ¹³C-MFA calculations depends strongly on the validity of several modeling assumptions that collectively form the basis for the underlying isotopomer models. These inherent assumptions include the following: (1) metabolic steady-state assumption—it is assumed that metabolic fluxes are constant during the labeling experiment; (2) isotopic steady-state assumption—it is assumed that isotopic labeling does not change in time; (3) no kinetic isotope effect for ¹³C tracers—it is assumed that enzymes cannot discriminate between unlabeled (¹²C) and labeled (¹³C) atoms^{83,93}; (4) no metabolite channeling—it is assumed that substrate tunneling via multi-enzyme complexes can be ignored; (5) homogeneous metabolite pools—it is assumed that metabolites within a particular compartment are perfectly mixed; (6) homogeneous cell population—it is assumed that all cells in a culture have the same metabolic phenotype; and (7) no turnover of macromolecules—it is assumed that cellular macromolecules such as proteins, lipids, RNA, and DNA are not broken down and produced at the same time. If one or more of these assumptions are shown to be incorrect for a given biological system, then the ¹³C-MFA methodology must be adjusted to account for these effects. For example, the isotopic ¹³C-NMFA was developed for analysis of systems where labeling data are not constant in time^{41,94}, and dynamic MFA methodologies (DMFA and ¹³C-DMFA) were developed for analysis of systems where fluxes are not constant in time^{46,95–97}. More recently, the co-culture ¹³C-MFA methodology was developed for analysis of non-homogeneous cell cultures⁸⁹. Turnover of macromolecules such as glycogen, lipids, and RNA has also been observed in many biological systems^{98–100}, and these effects can be captured in ¹³C-MFA by adding appropriate dilution fluxes⁹⁹.

Lastly, we want to emphasize the importance of full transparency in reporting ¹³C-MFA results by providing full access to data, models, methods, results, and statistics. As described in this review, ¹³C-MFA results are highly dependent on assumptions and models used for data analysis. As cancer research progresses and new insights are obtained into the unique metabolic features of cancer cells, we may discover additional reactions or pathways that have not been considered before. Reanalyzing past data using updated metabolic models could provide a powerful approach for testing new hypotheses. A recent review paper has proposed minimum data standards to facilitate dissemination of methods, data, and results from ¹³C-MFA studies⁴⁴.

Acknowledgements

This work was supported by NSF MCB-1616332 grant.

Conflict of interest

The authors declare that they have no conflict of interest.

Publisher's note

Springer Nature remains neutral with regard to jurisdictional claims in published maps and institutional affiliations.

Received: 6 December 2017 Accepted: 21 December 2017.

Published online: 16 April 2018

References

- DeBerardinis, R. J. & Thompson, C. B. Cellular metabolism and disease: what do metabolic outliers teach us? *Cell* **148**, 1132–1144 (2012).
- Metallo, C. M. & Vander Heiden, M. G. Understanding metabolic regulation and its influence on cell physiology. *Mol. Cell* **49**, 388–398 (2013).
- Dong, W., Keibler, M. A. & Stephanopoulos, G. Review of metabolic pathways activated in cancer cells as determined through isotopic labeling and network analysis. *Metab. Eng.* **43**, 113–124 (2017).
- Badur, M. G. & Metallo, C. M. Reverse engineering the cancer metabolic network using flux analysis to understand drivers of human disease. *Metab. Eng.* **45**, 95–108 (2017).
- Metallo, C. M. & DeBerardinis, R. J. Engineering approaches to study cancer metabolism. *Metab. Eng.* **43**, 93 (2017).
- Hiller, K. & Metallo, C. M. Profiling metabolic networks to study cancer metabolism. *Curr. Opin. Biotechnol.* **24**, 60–68 (2013).
- Boroughs, L. K. & DeBerardinis, R. J. Metabolic pathways promoting cancer cell survival and growth. *Nat. Cell Biol.* **17**, 351–359 (2015).
- Vander Heiden, M. G. & DeBerardinis, R. J. Understanding the Intersections between metabolism and cancer biology. *Cell* **168**, 657–669 (2017).
- Warburg, O. On the origin of cancer cells. *Science* **123**, 309–314 (1956).
- Liberti, M. V. & Locasale, J. W. The Warburg effect: how does it benefit cancer cells? *Trends Biochem. Sci.* **41**, 211–218 (2016).
- Hanahan, D. & Weinberg, R. A. Hallmarks of cancer: the next generation. *Cell* **144**, 646–674 (2011).
- Pavlova, N. N. & Thompson, C. B. The emerging hallmarks of cancer metabolism. *Cell Metab.* **23**, 27–47 (2016).
- Metallo, C. M. et al. Reductive glutamine metabolism by IDH1 mediates lipogenesis under hypoxia. *Nature* **481**, 380–384 (2011).
- Vander Heiden, M. G. et al. Evidence for an alternative glycolytic pathway in rapidly proliferating cells. *Science* **329**, 1492–1499 (2010).
- Possemato, R. et al. Functional genomics reveal that the serine synthesis pathway is essential in breast cancer. *Nature* **476**, 346–350 (2011).
- DeBerardinis, R. J. Serine metabolism: some tumors take the road less traveled. *Cell Metab.* **14**, 285–286 (2011).
- Pacold, M. E. et al. A PHGDH inhibitor reveals coordination of serine synthesis and one-carbon unit fate. *Nat. Chem. Biol.* **12**, 452–458 (2016).
- Locasale, J. W. Serine, glycine and one-carbon units: cancer metabolism in full circle. *Nat. Rev. Cancer* **13**, 572–583 (2013).
- Yang, M. & Vousden, K. H. Serine and one-carbon metabolism in cancer. *Nat. Rev. Cancer* **16**, 650–662 (2016).
- Coy, J. F., Dressler, D., Wilde, J. & Schubert, P. Mutations in the transketolase-like gene TKTL1: clinical implications for neurodegenerative diseases, diabetes and cancer. *Clin. Lab.* **51**, 257–273 (2005).
- Diaz-Moralli, S. et al. A key role for transketolase-like 1 in tumor metabolic reprogramming. *Oncotarget* **7**, 51875–51897 (2016).
- Schug, Z. T. et al. Acetyl-CoA synthetase 2 promotes acetate utilization and maintains cancer cell growth under metabolic stress. *Cancer Cell* **27**, 57–71 (2015).
- Mashimo, T. et al. Acetate is a bioenergetic substrate for human glioblastoma and brain metastases. *Cell* **159**, 1603–1614 (2014).
- Comerford, S. A. et al. Acetate dependence of tumors. *Cell* **159**, 1591–1602 (2014).
- Kamphorst, J. J., Chung, M. K., Fan, J. & Rabinowitz, J. D. Quantitative analysis of acetyl-CoA production in hypoxic cancer cells reveals substantial contribution from acetate. *Cancer Metab.* **2**, 23 (2014).
- Davidson, S. M. et al. Environment impacts the metabolic dependencies of Ras-driven non-small cell lung cancer. *Cell Metab.* **23**, 517–528 (2016).
- Achreja, A. et al. Exo-MFA—a ¹³C metabolic flux analysis framework to dissect tumor microenvironment-secreted exosome contributions towards cancer cell metabolism. *Metab. Eng.* **43**(Pt B), 156–172 (2017).
- Hensley, C. T. et al. Metabolic heterogeneity in human lung tumors. *Cell* **164**, 681–694 (2016).
- Patra, K. C. & Hay, N. The pentose phosphate pathway and cancer. *Trends Biochem. Sci.* **39**, 347–354 (2014).
- Nilsson, A. & Nielsen, J. Genome scale metabolic modeling of cancer. *Metab. Eng.* **43**, 103–112 (2017).
- Thiele, I. et al. A community-driven global reconstruction of human metabolism. *Nat. Biotechnol.* **31**, 419–425 (2013).
- Swarup, A., Lu, J., DeWoody, K. C. & Antoniewicz, M. R. Metabolic network reconstruction, growth characterization and ¹³C-metabolic flux analysis of the extremophile *Thermus thermophilus* HB8. *Metab. Eng.* **24**, 173–180 (2014).
- Long, C. P. & Antoniewicz, M. R. Metabolic flux analysis of *Escherichia coli* knockouts: lessons from the Keio collection and future outlook. *Curr. Opin. Biotechnol.* **28**, 127–133 (2014).
- Haverkorn van Rijsewijk, B. R., Nanchen, A., Nallet, S., Kleijn, R. J. & Sauer, U. Large-scale ¹³C-flux analysis reveals distinct transcriptional control of respiratory and fermentative metabolism in *Escherichia coli*. *Mol. Syst. Biol.* **7**, 477 (2011).
- Young, J. D. Metabolic flux rewiring in mammalian cell cultures. *Curr. Opin. Biotechnol.* **24**, 1108–1115 (2013).
- Jiang, L. et al. Reductive carboxylation supports redox homeostasis during anchorage-independent growth. *Nature* **532**, 255–258 (2016).
- Templeton, N. et al. Application of (¹³C) flux analysis to identify high-productivity CHO metabolic phenotypes. *Metab. Eng.* **43**(Pt B), 218–225 (2017).
- Maier, K. et al. Quantification of statin effects on hepatic cholesterol synthesis by transient (¹³C)-flux analysis. *Metab. Eng.* **11**, 292–309 (2009).
- Antoniewicz, M. R., Kelleher, J. K. & Stephanopoulos, G. Elementary metabolite units (EMU): a novel framework for modeling isotopic distributions. *Metab. Eng.* **9**, 68–86 (2007).
- Antoniewicz, M. R., Kelleher, J. K. & Stephanopoulos, G. Determination of confidence intervals of metabolic fluxes estimated from stable isotope measurements. *Metab. Eng.* **8**, 324–337 (2006).
- Young, J. D., Walther, J. L., Antoniewicz, M. R., Yoo, H. & Stephanopoulos, G. An elementary metabolite unit (EMU) based method of isotopically non-stationary flux analysis. *Biotechnol. Bioeng.* **99**, 686–699 (2008).
- Yoo, H., Antoniewicz, M. R., Stephanopoulos, G. & Kelleher, J. K. Quantifying reductive carboxylation flux of glutamine to lipid in a brown adipocyte cell line. *J. Biol. Chem.* **283**, 20621–20627 (2008).
- Young, J. D. INCA: a computational platform for isotopically non-stationary metabolic flux analysis. *Bioinformatics* **30**, 1333–1335 (2014).
- Crown, S. B. & Antoniewicz, M. R. Publishing ¹³C metabolic flux analysis studies: a review and future perspectives. *Metab. Eng.* **20**, 42–48 (2013).
- Crown, S. B. & Antoniewicz, M. R. Parallel labeling experiments and metabolic flux analysis: Past, present and future methodologies. *Metab. Eng.* **16**, 21–32 (2013).
- Antoniewicz, M. R. Methods and advances in metabolic flux analysis: a mini-review. *J. Ind. Microbiol. Biotechnol.* **42**, 317–325 (2015).
- Ahn, W. S. & Antoniewicz, M. R. Towards dynamic metabolic flux analysis in CHO cell cultures. *Biotechnol. J.* **7**, 61–74 (2012).
- Antoniewicz, M. R., Stephanopoulos, G. & Kelleher, J. K. Evaluation of regression models in metabolic physiology: predicting fluxes from isotopic data without knowledge of the pathway. *Metabolomics* **2**, 41–52 (2006).
- Crown, S. B., Long, C. P. & Antoniewicz, M. R. Optimal tracers for parallel labeling experiments and ¹³C metabolic flux analysis: a new precision and synergy scoring system. *Metab. Eng.* **38**, 10–18 (2016).
- Antoniewicz, M. R. ¹³C metabolic flux analysis: optimal design of isotopic labeling experiments. *Curr. Opin. Biotechnol.* **24**, 1116–1121 (2013).
- Buescher, J. M. et al. A roadmap for interpreting (¹³C) metabolite labeling patterns from cells. *Curr. Opin. Biotechnol.* **34**, 189–201 (2015).
- Schmidt, K., Carlsen, M., Nielsen, J. & Villadsen, J. Modeling isotopomer distributions in biochemical networks using isotopomer mapping matrices. *Biotechnol. Bioeng.* **55**, 831–840 (1997).
- Zupke, C. & Stephanopoulos, G. Intracellular flux analysis in hybridomas using mass balances and in vitro (¹³C) nmr. *Biotechnol. Bioeng.* **45**, 292–303 (1995).

54. Wiechert, W., Mollney, M., Isermann, N., Wurzel, M. & de Graaf, A. A. Bidirectional reaction steps in metabolic networks: III. Explicit solution and analysis of isotopomer labeling systems. *Biotechnol. Bioeng.* **66**, 69–85 (1999).
55. Ahn, W. S. & Antoniewicz, M. R. Metabolic flux analysis of CHO cells at growth and non-growth phases using isotopic tracers and mass spectrometry. *Metab. Eng.* **13**, 598–609 (2011).
56. Ahn, W. S. & Antoniewicz, M. R. Parallel labeling experiments with [1,2-(13C)] glucose and [U-(13C)] glutamine provide new insights into CHO cell metabolism. *Metab. Eng.* **15**, 34–47 (2013).
57. Crown, S. B., Ahn, W. S. & Antoniewicz, M. R. Rational design of (1)(3)C-labeling experiments for metabolic flux analysis in mammalian cells. *BMC Syst. Biol.* **6**, 43 (2012).
58. Metallo, C. M., Walther, J. L. & Stephanopoulos, G. Evaluation of 13C isotopic tracers for metabolic flux analysis in mammalian cells. *J. Biotechnol.* **144**, 167–174 (2009).
59. Antoniewicz, M. R. Parallel labeling experiments for pathway elucidation and 13C metabolic flux analysis. *Curr. Opin. Biotechnol.* **36**, 91–97 (2015).
60. Crown, S. B., Kelleher, J. K., Rouf, R., Muoio, D. M. & Antoniewicz, M. R. Comprehensive metabolic modeling of multiple 13C-isotopomer data sets to study metabolism in perfused working hearts. *Am. J. Physiol. Heart Circ. Physiol.* **311**, H881–H891 (2016).
61. DeWaal, D. et al. Hexokinase-2 depletion inhibits glycolysis and induces oxidative phosphorylation in hepatocellular carcinoma and sensitizes to metformin. *Nat. Commun.* **9**, 446 (2018).
62. Crown, S. B., Marze, N. & Antoniewicz, M. R. Catabolism of branched chain amino acids contributes significantly to synthesis of odd-chain and even-chain fatty acids in 3T3-L1 adipocytes. *PLoS ONE* **10**, e0145850 (2015).
63. Crown, S. B., Long, C. P. & Antoniewicz, M. R. Integrated 13C-metabolic flux analysis of 14 parallel labeling experiments in *Escherichia coli*. *Metab. Eng.* **28**, 151–158 (2015).
64. Long, C. P., Gonzalez, J. E., Sandoval, N. R. & Antoniewicz, M. R. Characterization of physiological responses to 22 gene knockouts in *Escherichia coli* central carbon metabolism. *Metab. Eng.* **37**, 102–113 (2016).
65. Long, C. P. & Antoniewicz, M. R. Quantifying biomass composition by gas chromatography/mass spectrometry. *Anal. Chem.* **86**, 9423–9427 (2014).
66. McConnell, B. O. & Antoniewicz, M. R. Measuring the composition and stable-isotope labeling of algal biomass carbohydrates via gas chromatography/mass spectrometry. *Anal. Chem.* **88**, 4624–4628 (2016).
67. Long, C. P., Au, J., Sandoval, N. R., Gebreselassie, N. A. & Antoniewicz, M. R. Enzyme I facilitates reverse flux from pyruvate to phosphoenolpyruvate in *Escherichia coli*. *Nat. Commun.* **8**, 14316 (2017).
68. Nakahigashi, K. et al. Systematic phenome analysis of *Escherichia coli* multiple-knockout mutants reveals hidden reactions in central carbon metabolism. *Mol. Syst. Biol.* **5**, 306 (2009).
69. Cordova, L. T., Cipolla, R. M., Swarup, A., Long, C. P. & Antoniewicz, M. R. (13C) metabolic flux analysis of three divergent extremely thermophilic bacteria: *Geobacillus* sp. LC300, *Thermus thermophilus* HB8, and *Rhodothermus marinus* DSM 4252. *Metab. Eng.* **44**, 182–190 (2017).
70. Clasquin, M. F. et al. Riboneogenesis in yeast. *Cell* **145**, 969–980 (2011).
71. Crown, S. B. et al. Resolving the TCA cycle and pentose-phosphate pathway of *Clostridium acetobutylicum* ATCC 824: isotopomer analysis, in vitro activities and expression analysis. *Biotechnol. J.* **6**, 300–305 (2011).
72. Feng, X. et al. Characterization of the central metabolic pathways in *Thermoanaerobacter* sp. strain X514 via isotopomer-assisted metabolite analysis. *Appl. Environ. Microbiol.* **75**, 5001–5008 (2009).
73. Ahn, W. S., Crown, S. B. & Antoniewicz, M. R. Evidence for transketolase-like TKTL1 flux in CHO cells based on parallel labeling experiments and (13)C-metabolic flux analysis. *Metab. Eng.* **37**, 72–78 (2016).
74. Kharroubi, A. T., Masterson, T. M., Aldaghas, T. A., Kennedy, K. A. & Kelleher, J. K. Isotopomer spectral analysis of triglyceride fatty acid synthesis in 3T3-L1 cells. *Am. J. Physiol.* **263**(4 Pt 1), E667–E675 (1992).
75. Green, C. R. et al. Branched-chain amino acid catabolism fuels adipocyte differentiation and lipogenesis. *Nat. Chem. Biol.* **12**, 15–21 (2016).
76. Fendt, S. M. et al. Metformin decreases glucose oxidation and increases the dependency of prostate cancer cells on reductive glutamine metabolism. *Cancer Res.* **73**, 4429–4438 (2013).
77. Jiang, L. et al. Quantitative metabolic flux analysis reveals an unconventional pathway of fatty acid synthesis in cancer cells deficient for the mitochondrial citrate transport protein. *Metab. Eng.* **43**(Pt B), 198–207 (2017).
78. Crown, S. B. & Antoniewicz, M. R. Selection of tracers for 13C-metabolic flux analysis using elementary metabolite units (EMU) basis vector methodology. *Metab. Eng.* **14**, 150–161 (2012).
79. DeBerardinis, R. J. et al. Beyond aerobic glycolysis: transformed cells can engage in glutamine metabolism that exceeds the requirement for protein and nucleotide synthesis. *Proc. Natl Acad. Sci. USA* **104**, 19345–19350 (2007).
80. Previs, S. F. et al. New methodologies for studying lipid synthesis and turnover: looking backwards to enable moving forwards. *Biochim. Biophys. Acta* **1842**, 402–413 (2014).
81. Landau, B. R. et al. Contributions of gluconeogenesis to glucose production in the fasted state. *J. Clin. Invest.* **98**, 378–385 (1996).
82. Hasenour, C. M. et al. Mass spectrometry-based microassay of (2)H and (13)C plasma glucose labeling to quantify liver metabolic fluxes in vivo. *Am. J. Physiol. Endocrinol. Metab.* **309**, E191–E203 (2015).
83. Sandberg, T. E. et al. Evolution of *E. coli* on [U-13C]glucose reveals a negligible isotopic influence on metabolism and physiology. *PLoS ONE* **11**, e0151130 (2016).
84. Liu, L. et al. Malic enzyme tracers reveal hypoxia-induced switch in adipocyte NADPH pathway usage. *Nat. Chem. Biol.* **12**, 345–352 (2016).
85. Lewis, C. A. et al. Tracing compartmentalized NADPH metabolism in the cytosol and mitochondria of mammalian cells. *Mol. Cell* **55**, 253–263 (2014).
86. Fan, J. et al. Quantitative flux analysis reveals folate-dependent NADPH production. *Nature* **510**, 298–302 (2014).
87. Wahrheit, J., Nicolae, A. & Heinzle, E. Eukaryotic metabolism: measuring compartment fluxes. *Biotechnol. J.* **6**, 1071–1085 (2011).
88. Niklas, J., Schneider, K. & Heinzle, E. Metabolic flux analysis in eukaryotes. *Curr. Opin. Biotechnol.* **21**, 63–69 (2010).
89. Gebreselassie, N. A. & Antoniewicz, M. R. (13)C-metabolic flux analysis of cocultures: a novel approach. *Metab. Eng.* **31**, 132–139 (2015).
90. Chen, W. W., Freinkman, E., Wang, T., Birsoy, K. & Sabatini, D. M. Absolute quantification of matrix metabolites reveals the dynamics of mitochondrial metabolism. *Cell* **166**, 1324–1337 e11 (2016).
91. Nicolae, A., Wahrheit, J., Nonnenmacher, Y., Weyler, C. & Heinzle, E. Identification of active elementary flux modes in mitochondria using selectively permeabilized CHO cells. *Metab. Eng.* **32**, 95–105 (2015).
92. Nonnenmacher, Y. et al. Analysis of mitochondrial metabolism in situ: combining stable isotope labeling with selective permeabilization. *Metab. Eng.* **43**, 147–155 (2017).
93. Wasylenko, T. M. & Stephanopoulos, G. Kinetic isotope effects significantly influence intracellular metabolite (13)C labeling patterns and flux determination. *Biotechnol. J.* **8**, 1080–1089 (2013).
94. Wiechert, W. & Noh, K. From stationary to instationary metabolic flux analysis. *Adv. Biochem. Eng. Biotechnol.* **92**, 145–172 (2005).
95. Antoniewicz, M. R. Dynamic metabolic flux analysis—tools for probing transient states of metabolic networks. *Curr. Opin. Biotechnol.* **24**, 973–978 (2013).
96. Leighty, R. W. & Antoniewicz, M. R. Dynamic metabolic flux analysis (DMFA): a framework for determining fluxes at metabolic non-steady state. *Metab. Eng.* **13**, 745–755 (2011).
97. Antoniewicz, M. R. et al. Metabolic flux analysis in a nonstationary system: fed-batch fermentation of a high yielding strain of *E. coli* producing 1,3-propanediol. *Metab. Eng.* **9**, 277–292 (2007).
98. Long, C. P., Au, J., Gonzalez, J. E. & Antoniewicz, M. R. 13C metabolic flux analysis of microbial and mammalian systems is enhanced with GC-MS measurements of glycogen and RNA labeling. *Metab. Eng.* **38**, 65–72 (2016).
99. Gonzalez, J. E., Long, C. P. & Antoniewicz, M. R. Comprehensive analysis of glucose and xylose metabolism in *Escherichia coli* under aerobic and anaerobic conditions by 13C metabolic flux analysis. *Metab. Eng.* **39**, 9–18 (2017).
100. Guzman, S. et al. (13)C metabolic flux analysis shows that resistin impairs the metabolic response to insulin in L6E9 myotubes. *BMC Syst. Biol.* **8**, 109 (2014).